

Analysis of ridges and grooves shape in a grating coupler for optimization of integrated optics sensor structures.

Przemysław Struk*

Department of Optoelectronics, Faculty of Electrical Engineering, Silesian University of Technology,
2 Krzywoustego Str. 44-100 Gliwice, Poland

Received May 15, 2022; accepted September 28, 2022; published September 30, 2022

Abstract—The paper presents a theoretical analysis of a sensor structure based on a planar waveguide and grating coupler designed to determine selected physical properties of blood – hemoglobin concentration and oxidation level. In particular, the analysis was focused on optimization of selected geometrical properties of a grating coupler (the shape of ridges and grooves) to obtain maximum efficiency of uncoupling of light from the sensor structure. The analysis was carried out for three types of ridges and grooves shape in a grating coupler: rectangular, triangular and sinusoidal.

Nowadays, medicine requires fast and accurate diagnostic methods for measurement of physical properties of biological liquids, especially properties of blood [1–2]. The knowledge about blood properties plays a key role in determining of the patient’s health condition [1–3]. From this point of view, modern medicine requires the development of new methods and sensor structures designed for measurement of blood properties including oxidation level and hemoglobin concentration [4–7]. The integrated optics structures based on a planar waveguide and a grating coupler offer attractive possibilities of application as a sensor structure for measurement of selected properties of biological liquids, including blood properties - oxidation and concentration of haemoglobin [7–10].

The presented sensor structure consists of a prism coupler for introduction of light generated by a laser into a structure, planar waveguide and grating coupler. The part of the structure with a planar waveguide is responsible for measurement of hemoglobin oxidation (changes in an imaginary part of refractive index k) thanks to the phenomena of evanescent field of the guided mode. The grating coupler is responsible for measurement of hemoglobin concentration (changes of real part of refractive index n). An additional task of the grating coupler feature is uncoupling light from the sensor structure to the detector. The mathematical equation describing uncoupling of light from a waveguide by a grating coupler is presented below [7, 9–10]:

$$\beta_c \sin(\alpha) = \beta_w + \frac{m_o 2\pi}{\Lambda}, \quad (1)$$

where: β_c , β_w – the propagation constant in the environment and waveguide respectively, Λ – the space period of the grating, m_o – the diffraction order, α – the angle of light uncoupling.

The angle α of light uncoupling from the structure can be written as [7–9]:

$$\alpha = \arcsin \left[\frac{1}{n_c} \left(N_{eff} - \frac{m_o \lambda}{\Lambda} \right) \right], \quad (2)$$

where: λ_0 – the wavelength, N_{eff} – the effective refractive index.

The schematic view of the sensor structure is presented in Fig. 1.

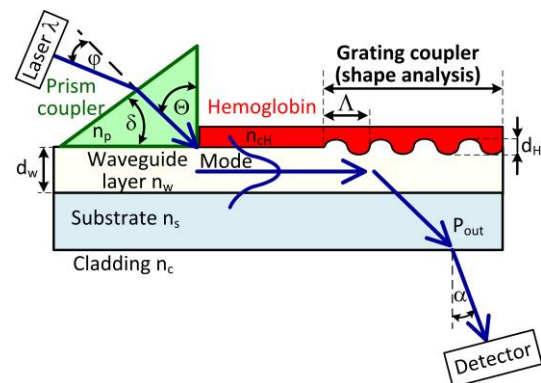


Fig. 1. The scheme of the sensor structure.

A detailed description of the principle of operation of the presented sensor structure and selected numerical analysis have been presented in the previous articles [7–8, 12].

Numerical analyses presented in the manuscript were focused on optimizing efficiency of light uncoupling by a grating coupler from structure to detector as a function of the grating coupler geometrical properties – shape of ridge and grooves. The numerical analysis of uncoupled power of light to substrate direction P_{out} was carried out for the following shapes of ridges and grooves in a grating coupler:

* E-mail: Przemyslaw.Struk@polsl.pl

– *rectangular shape* – the grating coupler with a height of ridges d_H is placed on the waveguide layer with thickness d_w (Fig. 2.a),

– *triangular shape* – the grating coupler with a height of ridges d_H placed on the waveguide layer with thickness d_w (Fig. 2.b),

– *sinusoidal shape* – the grating coupler with a height of ridges d_H into waveguide layer with thickness d_w (Fig. 2.c).

The numerical analyses were performed by using the Finite Difference Time Domain method (FDTD) in 2D. The wavelength of light $\lambda=560\text{nm}$ was chosen for ensure maximum sensitivity of the presented sensor structure for detection of hemoglobin physical properties [7].

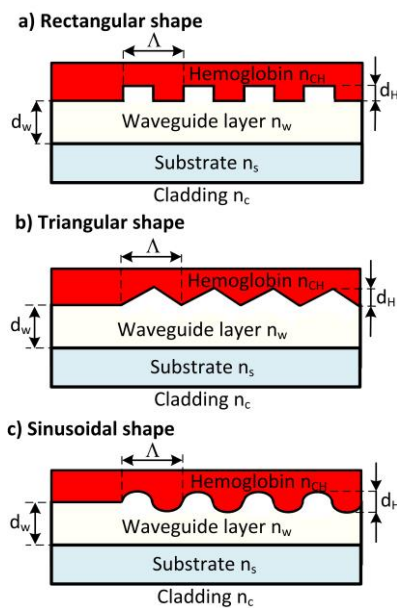


Fig. 2. Shape of ridges and grooves in grating coupler.

The key issue during the numerical analysis was to select the proper boundary conditions such as mesh size, time step and layers which surrounded the analysed area. The mesh size and time step were chosen to ensure the Courant–Friedrichs–Lewy condition and for a appropriate and accurate mapping of the grating coupler topography [13–14]. The mesh size on the x axis and z axis was equal to $\Delta x=2\text{nm}$, $\Delta z=2\text{nm}$ respectively, time step was equal to $\Delta t=4.44\text{e}^{-18}$ sec. The edge of the analysed area on the x and z axis was surrounded by anisotropic perfectly matched layers (APML). The optical properties – refractive index of each layer in the structure was as follows: waveguide layer $n_w=2.3$, substrate $n_s=1.465$ and hemoglobin $n_{CH}=1.3681$ (corresponding to hemoglobin level 17.3 g/dL) respectively [7]. The grating coupler had a spatial period equal to $\Lambda=600\text{nm}$ and periods numbers $N=25$.

The thickness of a waveguide layer has been chosen to correspond with maximum homogeneous sensitivity for waveguide modes and was equal to $d_w=188\text{nm}$ or $d_w=237\text{nm}$. A detailed analysis of the homogeneous sensitivity was presented in the previous paper [7].

The first analysis presented in the paper was carried out for the grating coupler with a ridge and grooves in the form of a rectangular shape. It should be noted that the periodic structure of grating (ridges and grooves) with thickness d_H was placed on the waveguide layer with thickness d_w Fig. 2a.

This is a different construction than the one presented in an earlier paper, where the periodic structure of a grating coupler was placed into the waveguide layer [12]. The calculated output power of light P_{out} as a function of grooves depth in a grating coupler for the sensor structure with waveguide layer thickness $d_w=188\text{nm}$ is presented in Fig. 3. The analysis of results shows that if the height of ridges increases, then the power of light uncoupled from the sensor structure through the grating coupler also increases up to a maximum value. The optimal ridges height d_H in a grating coupler is strongly dependent on waveguide mode polarization. The optimal height of ridges for TE₀₀ mode is at the level of $d_H=88\text{nm}$, while for TM₀₀ mode is at the level $d_H=76\text{nm}$. The distribution of the Poynting vector for TE₀₀ and TM₀₀ mode is presented in Fig. 4a and Fig.4b.

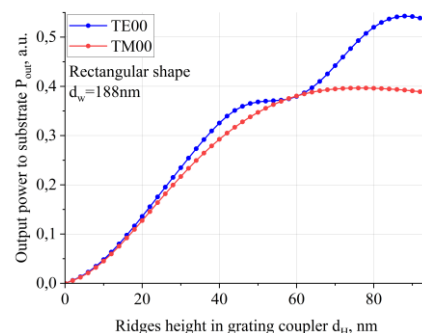


Fig. 3. The output power of light P_{out} transmitted to a substrate as a function of ridges height d_H for rectangular shape of ridge and grooves.

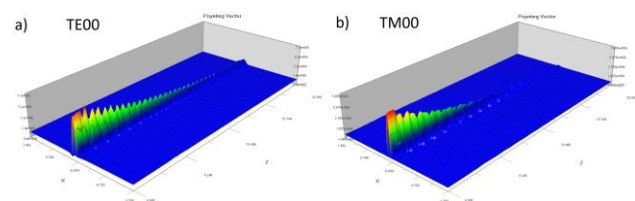


Fig. 4. Poynting vector for mode: a) TE₀₀, b) TM₀₀, $d_w=188\text{nm}$, $d_H=76\text{nm}$.

In the case of the sensor structure with a thickness of waveguide layer $d_w=237\text{nm}$, the power of light uncoupled from the structure P_{out} heavily depends on: polarization

and order of waveguide mode as a function of ridge height. Higher order modes such as: TE01 and TM01 are more sensitive to ridge height in a grating coupler than TE00 and TM00 modes. For a given ridge height, higher order modes TE01 and TM01 are uncoupled from the structure much more strongly than lower order modes TE00 and TM00 (Fig. 5). The optimal height of the ridge for TE00 and TM00 modes is around $d_H=70\text{nm}$, however the optimal height of ridge for TE01 is at the level of $d_H=44\text{nm}$.

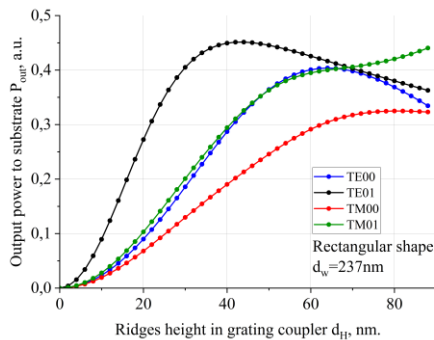


Fig. 5. The output power of light P_{out} transmitted to the substrate as a function of ridges height d_H for rectangular shape of the grating coupler.

In the case of a grating coupler with ridges and grooves of a triangular shape, the calculated uncoupled power of light P_{out} by a grating coupler for the structure with a waveguide layer thickness $d_w=188\text{nm}$ or $d_w=237\text{nm}$ is presented in Fig. 6 and Fig. 7, respectively. The P_{out} is growing with an increase in the height of ridges in a grating coupler. The light coupling efficiency for the structure with $d_w=188\text{nm}$ and grating with a triangular shape is lower than the other presented shapes for a given height of grooves. The distribution of the Poynting vector for TE00 and TM00 mode is presented in Fig. 8a and Fig. 8b, respectively.

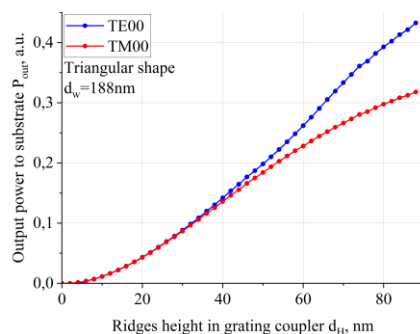


Fig. 6. The output power of light P_{out} transmitted to the substrate as a function of ridges height d_H for triangular shape of the grating coupler.

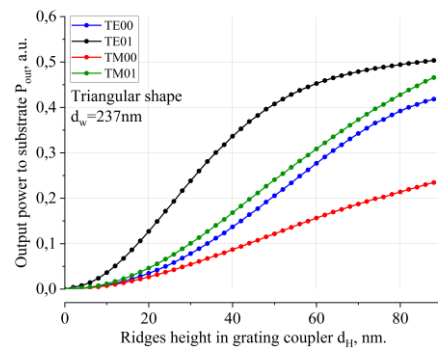


Fig. 7. The output power of light P_{out} transmitted to the substrate as a function of ridges height d_H for triangular shape of the grating coupler.

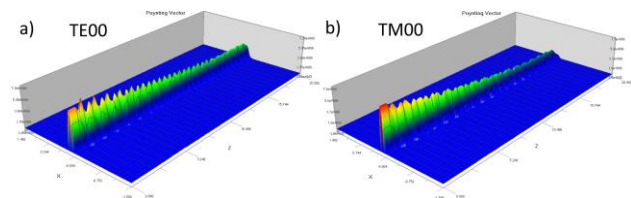


Fig. 8. Poynting vector for mode: a) TE00, b) TM00, $d_w=188\text{nm}$, $d_H=80\text{nm}$.

The results of a numerical analysis for the sensor structure with a sinusoidal shape of ridges and grooves in the grating coupler and with waveguide layer thickness $d_w=188\text{nm}$ are presented below. The maximum uncoupled power of light P_{out} is for the depth of grooves height $d_H=88\text{nm}$ for TE00 and $d_H=104\text{nm}$ for TM00 modes Fig. 9. The output power P_{out} is a little bit higher than the earlier presented shape of ridges and grooves in grating couplers.

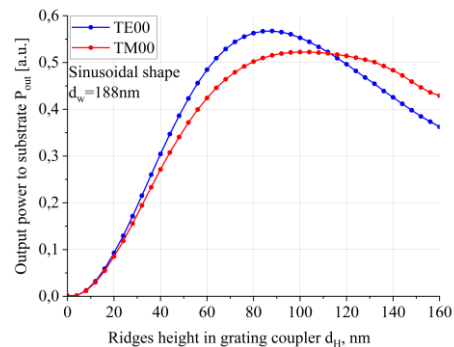


Fig. 9. The output power of light P_{out} transmitted to the substrate as a function of ridges height d_H for sinusoidal shape of the grating coupler.

The distribution of the Poynting vector for selected waveguide modes TE00 and TM00 into the structure are presented in Fig. 10a and Fig. 10b, respectively.

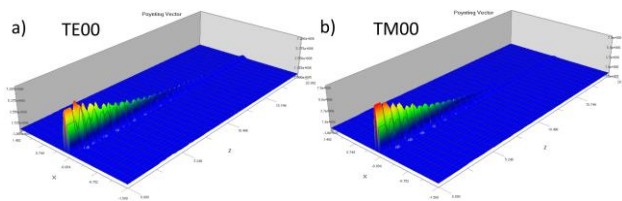


Fig. 10. Poynting vector mode: a) TE00, b) TM00, $d_w=188\text{nm}$, $d_H=90\text{nm}$.

The numerical analyses presented below are focused on the grating coupler with a sinusoidal shape of ridges and grooves and the waveguide layer thickness $d_w=237\text{nm}$. The power of light P_{out} uncoupled from the sensor structure as a function of ridge and grooves height d_H is heavily depends on polarization and waveguide mode order. The TE polarization modes are more sensitive to ridge height in a grating coupler than TM polarization modes. Generally, for given ridges and grooves, height d_H modes with polarization TE00 and TE01 are uncoupled from the structure much more strongly than the modes with polarization TM00 and TM01 (Fig. 11). The maximum of uncoupled optical power from the structure by a grating coupler is observed for lower ridge heights d_H for TE modes than TM.

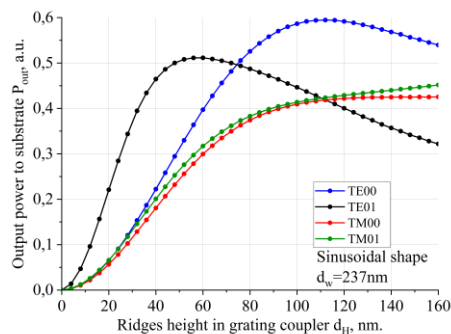


Fig. 11. The output power of light P_{out} transmitted to the substrate as a function of ridges height d_H for sinusoidal shape of the grating coupler.

The optimal height of the ridges and grooves for waveguide mode TE00 is $d_H=112\text{nm}$, in the case of TE01 mode, $d_H=60\text{nm}$. In the case of modes TM00 and TM01, the optimal depth is around $d_H=160\text{nm}$.

Numerical analyses showed a heavy dependence of grating coupler efficiency for light uncoupling as a function of ridges and grooves shape and height.

In addition, the analyses showed a great dependence of uncoupled power of light on the grating coupler as a function of waveguide modes polarization and its order. The optimal shape and height of periods in a grating coupler should be designed for strictly defined properties of sensor structure such as refractive index distribution in structure and hence effective refractive index, layers

thickness, spatial period of grating, periods number, wavelength of light, polarization of waveguide mode, waveguide mode order and maximum homogenous sensitivity.

If we know which waveguide mode we would like to use (based on analysis of homogenous sensitivity) in the designed sensor structure, then we should take into account the results of the numerical analysis presented below. However, if we make an assumption the grating coupler should be useful for a wide range of waveguide modes and waveguide mode polarizations, then, as numerical analysis showed, the periods height should be around $60\text{nm}-80\text{nm}$.

The numerical analyses were carried out on a computer financed by the Silesian University of Technology Rector's pro-quality grant: 05/040/RGJ20/2003.

References

- [1] I. Singh, A. Weston, A. Kundur, G. Dobie, *Haematology Case Studies with Blood Cell Morphology and Pathophysiology* (Elsevier Amsterdam, The Netherlands 2017).
- [2] P. Jarolim, M. Lahav, S.C. Liu, J. Palek, *Blood* **76**, 10(1990).
- [3] E. Beutler, J. Waalen, *Blood* **107**, 5 (2006).
- [4] M. Kiroriwal, P. Singal, M. Sharma, A. Singal, *Opt. Laser Techn.* **149**, 107817 (2022).
- [5] A.A. Boiarski, J.R. Busch, B.S. Bhullar, R.W. Ridgway, V.E. Wood, *Proc. SPIE Integrated Optics and Microstructures* **1793**, 199(1993).
- [6] L. Cheng, S. Mao, Z. Li, Y. Han, H. Y. Fu, *Micromachines* **11**, 666 (2020).
- [7] P. Struk, *Materials* **12**, 175 (2019).
- [8] P. Struk, *Phot. Lett. Poland* **12**, 2 (2020).
- [9] P.V. Lambeck, *Meas. Sci. Technol.* **17**(8), R93(2006).
- [10] W. Lukosz, *Sens. Actuators B Chem* **29**(1-3), 37(1995).
- [11] P. Struk, T. Pustelny, K. Gołaszewska, E. Kaminska, M.A. Borysiewicz, M. Ekielski, A. Piotrowska, *Opto-Electron. Rev.* **21**, 376 (2013).
- [12] P. Struk, *Proc. SPIE* **11204**, 1120401-1 (2019).
- [13] *OptiFDTD Technical Background and Tutorials - Finite Difference Time Domain Photonics Simulation Software*, Optiwave Systems Inc. (2008).
- [14] K. Yee, *IEEE Transactions* **14**, 3 (1966).